

Design and pressure analysis for bulk-micromachined electrothermal hydraulic microactuators using a PCM

Jun Su Lee*, Stepan Lucyszyn

Optical and Semiconductor Devices Group, Department of Electrical and Electronic Engineering, Imperial College London, Exhibition Road, London SW7 2AZ, United Kingdom

Received 8 July 2005; received in revised form 10 January 2006; accepted 15 May 2006
Available online 18 July 2006

Abstract

Paraffin wax exhibits a volumetric expansion of $\sim 15\%$, at around its melting point. By exploiting this phenomenon, high performance bulk-machined electrothermal hydraulic microactuators have been demonstrated. The microactuators have been integrated into microfluidic valves, microgrippers and micropipettes. The paraffin wax is confined within a bulk-micromachined silicon container. This container is sealed using an elastic diaphragm of PDMS, while it is heated via gold microheaters located on an underlying glass substrate. All the layers used to make up the containers are bonded together using a unique combination of overglaze paste and PDMS. The hydraulic pressure of expanding paraffin wax was determined using the deflection theory of a circular plate. For the first time, the hydraulic pressure of expanding paraffin wax was calculated using the theory of large deflections for a circular plate and measured data from the type-A microgripper. This theory has been exploited for the deflection analysis of micromachined thin elastic diaphragms. In order to calculate the hydraulic pressure, the theory of large deflections of a circular plate is calculated using the measured actuation height, the PDMS diaphragm dimension of the microgripper (type-A) and mechanical properties of the PDMS. The hydraulic pressure was calculated to be approximately 0.12 MPa. All the devices were successfully demonstrated and operated at either 10 or 15 V. © 2006 Elsevier B.V. All rights reserved.

Keywords: Paraffin wax microactuator; Microvalve; Microgripper; Micropipette; Hydraulic pressure

1. Introduction

With microactuators, various physical phenomena have been exploited. One of the most powerful forms of actuation is obtained by using phase change materials (PCMs). PCMs have the property of volumetric expansion when changing from solid to liquid (or liquid to gas) phases. This expansion can produce large hydraulic pressures that can be exploited to realise useful electrothermal microactuators, when compared to other types of microactuators as shown in Fig. 1 [1].

As a PCM, paraffin wax is a suitable actuation material because when paraffin wax melts a volumetric expansion of $\sim 15\%$ occurs, as illustrated in Fig. 2(a) [2]. Since paraffin wax can produce a very large force, under expansion, this hydraulic force has been exploited by microactuators used in linear micropositioners [3,4] and for the manipulation of surgical instruments [5]. In recent years, surface-micromachined

microactuators and valves [6–8] have been developed. However, even though the paraffin wax microactuator offers many possibilities, its applications have not been widely demonstrated. The authors have recently demonstrated the practical realization of this microactuator in a refreshable Braille cell [9]. However, this paper, presents new applications for this hydraulic microactuator in microfluidic valves, microgrippers and micropipettes.

Unlike the surface-micromachining version [6,8], our bulk-micromachining microactuators have containers for the paraffin wax, to allow design flexibility for extended performance. It consists of a microheater, bulk-micromachined container and polydimethylsiloxane (PDMS) diaphragm, as illustrated in Fig. 2(b and c).

This microactuator can be used directly as a microfluidic valve, since the structure of the device is relatively simple and a high integrity seal is inherent. The valve closes a microchannel, by means of expansion of the melting paraffin wax, and opens, by means of contraction of the solidifying paraffin wax. The microvalve unit consists of two microactuators, positioned in the two opposite outlet channels.

* Corresponding author. Tel.: +44 20 7594 6167; fax: +44 20 7594 6308.
E-mail address: jun-su.lee@imperial.ac.uk (J.S. Lee).

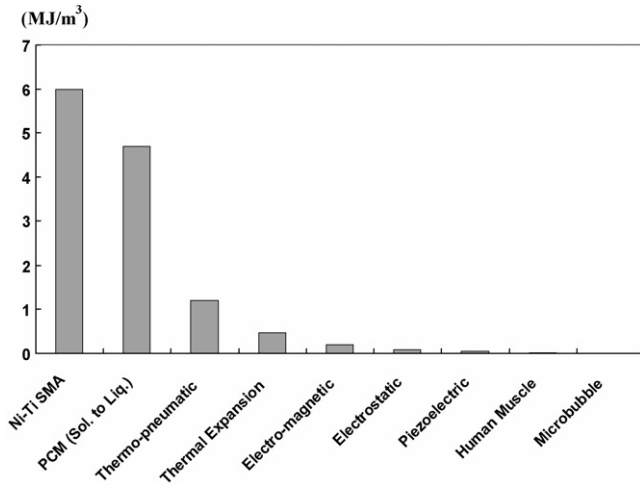


Fig. 1. Work per unit volume for various microactuator types [1].

The microgripper can also be driven using the paraffin wax microactuator. Two actuation modes are described here. The microgripper can be closed with the actuation from the outside to the inside of the gripper (type-A), or be opened with the microactuator operation from the inside to the outside (type-B).

The last application is the micropipette, used for sampling small quantities of liquids. A liquid is drawn-in by creating a

low pressure within the micropipette’s chamber, and then the liquid is expelled by creating a high pressure within the chamber. The paraffin wax microactuators can generate the low and high pressures by the respective shrinkage and expansion of the paraffin wax.

For the first time, this paper describes the design and fabrication of the paraffin wax microactuators and its new applications within microvalves, microgrippers (type-A and B) and micropipettes. In addition, the hydraulic expansion pressure of molten paraffin wax is calculated using the theory of large deflection.

2. Design and fabrication

Under normal conditions, the PDMS diaphragm expands into a hemispherical shape when the microactuator is actuated. The height of the hemisphere defines the displacement of the microactuator. If the microactuator is required for a specific height of actuation, the diameter of the bottom circle of the hemisphere is determined by considering the entire size of the microactuator. The volume of the expanded paraffin wax can be calculated from the dimensions of the hemisphere. Using the expanded volume, the solid phase volumes for the paraffin wax and the container dimensions can be also calculated, since an expansion of 15% is expected. However, the expanded hemisphere is not a perfect hemisphere but a dome, as illustrated by the shaded area in Fig. 3. With the dimensions given in Fig. 3, the volume of the hemispherical dome can be calculated using the following volume integral:

$$V_{\text{dome}} = \pi \int_a^b (r^2 - x^2) dx \tag{1}$$

where the specific height of the displacement for the actuation is h , and r is a spherical radius from the given bottom diameter. Since the dome is part of a perfect hemisphere on the x - y axis, the limits of the integral, a and b , are shown as points on the x axis. Using (1), the volume of the hemispherical dome, therefore, can be easily calculated. Because the calculated volume of the hemisphere is 15 vol.% of the solidified paraffin wax. The volume of solid paraffin wax and the container dimensions can also be obtained. In this work, the displacement heights of 200, 300 and 500 μm are required for the microvalves, microgrippers and micropipettes, respectively.

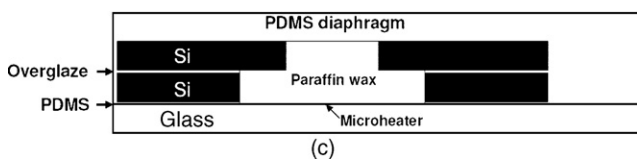
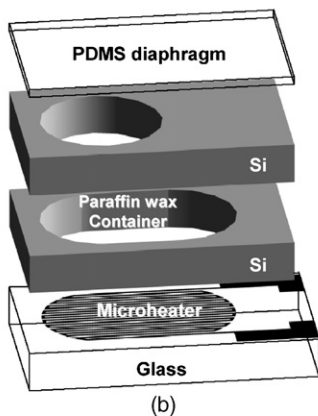
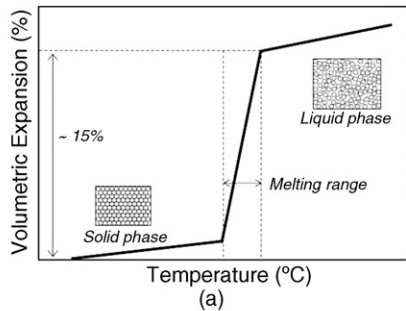


Fig. 2. (a) Typical volumetric expansion curve of paraffin wax, (b) exploded view of the basic bulk-micromachined microactuator and (c) cross-sectional view of the microactuator.

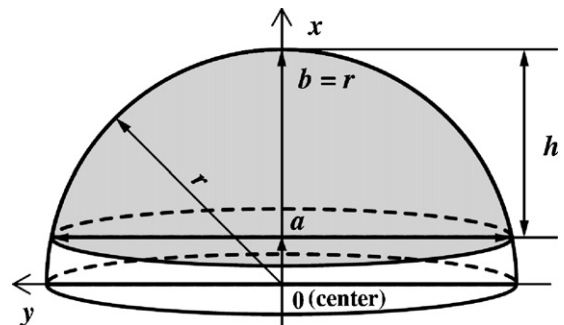


Fig. 3. Dimensions of the actuated hemisphere.

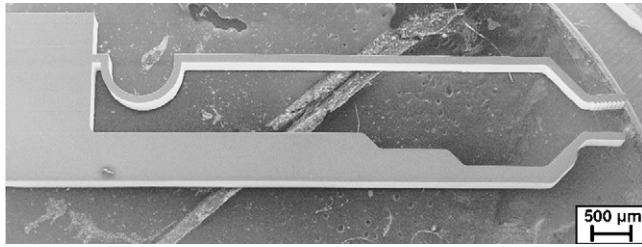


Fig. 4. Silicon bulk-micromachined microgripper (type-A) using DRIE.

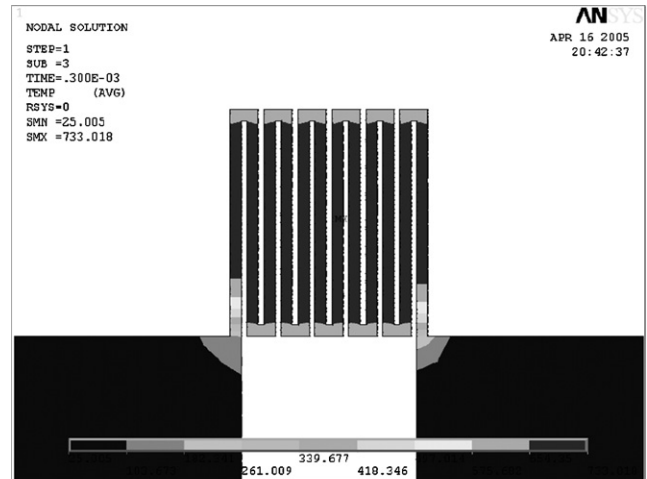
With a silicon wafer ($\sim 525 \mu\text{m}$ thickness), the containers for the microactuator, microgripper and micropipette chambers were fabricated using deep reactive ion etching (DRIE), which permits the etching of vertical side walls and high-aspect-ratio silicon structures. A photoresist (AZ9260) was spin-coated onto the silicon wafer, with a thickness of $\sim 15 \mu\text{m}$, and patterned photolithographically. A dummy wafer was attached using thermal conductive grease to the patterned wafer for support. This silicon wafer was DRIE etched for 3 h 30 min. The fabricated silicon element for a microgripper is shown in Fig. 4.

Microheaters can generate enough thermal energy, through Joules heating. The metal microheaters were realized by depositing gold (Au) tracks on a glass (Pyrex) substrate. Since glass has very low thermal conductivity, thermal loss by conduction through the substrate can be minimized. A high density microheater covers the entire underside of the container, having a thickness of 3000 \AA and a width of $50 \mu\text{m}$. Using the finite element numerical simulation software of ANSYS, the heating performance of the microheater was undertaken before fabrication, as shown in Fig. 5(a).

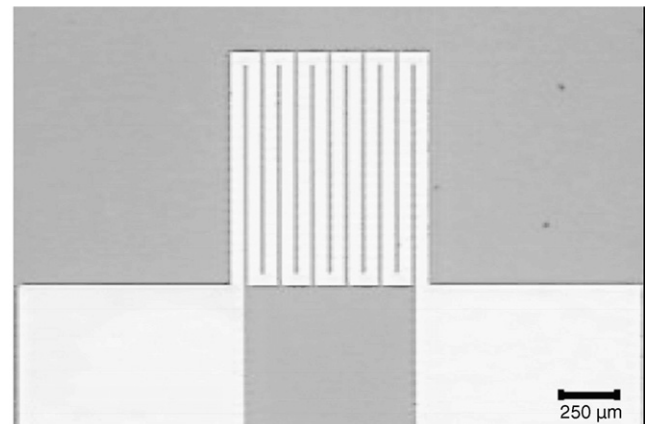
At first, a 250 \AA thick chromium (Cr) layer was RF sputter-coated onto the glass wafer for the adhesion of the gold layer. Gold was then sputter-coated onto the Cr layer, with a thickness of 3000 \AA . A thin photoresist (S1813) was deposited using a spin-coater and baked at 100°C for 2 min on a hotplate. Then, the heater was patterned photolithographically. The Au and Cr layer was etched using Au and Cr etchants, respectively. Fig. 5(b) shows an optical microscope image of the microheater.

Each component of the microactuator was bonded using an overglaze paste and a room temperature curing PDMS. The two silicon layers were attached together using the overglaze paste (Dupont, QQ550), and then fired in a furnace at 550°C for 10 min in air. During firing, the overglaze's glass frit powder is sintered and forms a bonding layer, with the sintered overglaze completely sealing gaps at the interfaces, as show in Fig. 6. The bonded silicon containers were attached to the glass using PDMS.

The containers were filled with paraffin wax using on a hot-plate heated to $\sim 50^\circ\text{C}$. The paraffin wax was injected into the containers in a molten state. After solidifying, the almost-filled containers were topped-up using very small volumes of solid paraffin wax. The top of the microactuator was covered with PDMS. Here, at the room temperature, the PDMS paste was pressed using a glass slide to form a thin and flat diaphragm. Although the thicknesses of the diaphragms were not perfectly uniform, the average thickness was approximately $77 \mu\text{m}$.



(a)



(b)

Fig. 5. (a) Electrothermal 3D simulation for a gold microheater (5 V for 1 s) and (b) optical microscopy fabricated microheater.

The microchannel of the microvalve was fabricated using SU-8 2050. A $150 \mu\text{m}$ thick SU-8 layer was spin-coated (1200 rpm for 30 s) on a glass wafer. It was soft-baked at 65°C for 5 min and 95°C for 20 min. This wafer was exposed at 600 mJ/cm^2 and then post-baked at 65°C for 1 min and 95°C for 12 min. The microchannels-on-glass were cut as one unit microchannel, and the unit microchannel was bonded onto the microvalve microactuators.

For the last step of the assembly process, the bulk-micromachined silicon microgrippers and micropipette chambers were bonded onto the fabricated microactuators using PDMS. With the micropipette, a glass plate covered the chamber and a glass tube (o.d./i.d.: 1/0.58 mm) was connected to the chamber. All of these components have been bonded and sealed using PDMS. Fig. 7 shows the completed microvalve, microgripper and micropipette.

3. Measured results

3.1. Microvalve

In order to measure and observe the driving performance, these devices were placed under an optical microscope and

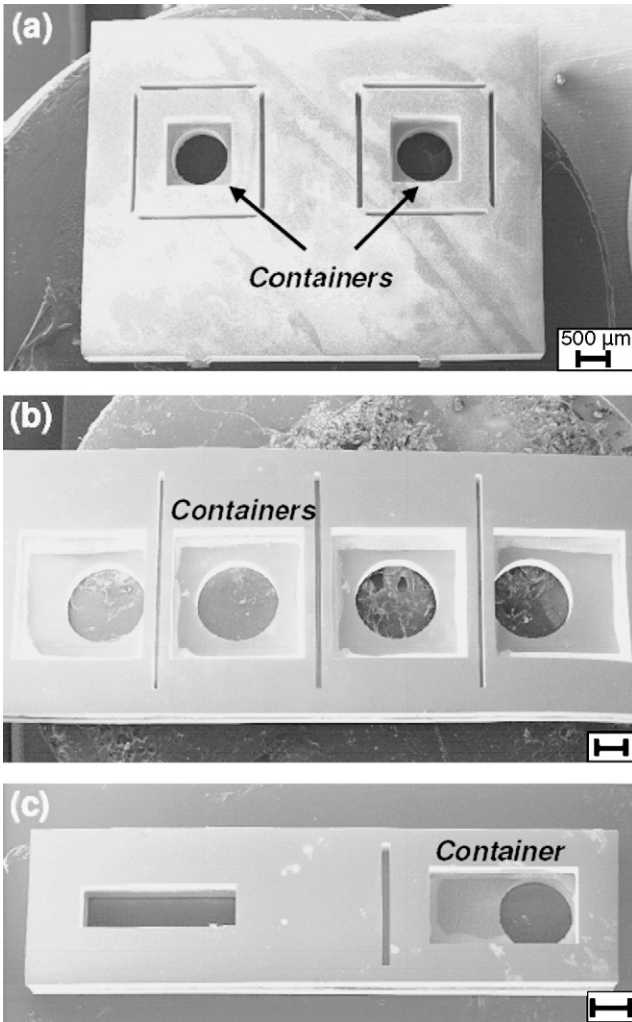
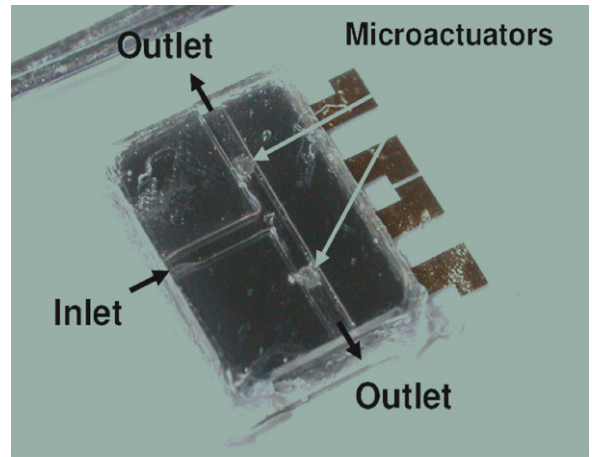


Fig. 6. Underside view of the bonded silicon layers that make up the containers for the: (a) microfluidic valve, (b) micropipette and (c) microgripper.

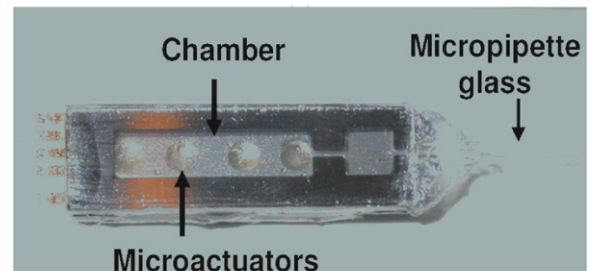
the control bias voltage was applied via dc probe needles. The microfluidic valve has a T-shape microchannel, consisting of one inlet and two outlets. The dimensions for the microchannel are: height, $\sim 150 \mu\text{m}$ and width, $700 \mu\text{m}$. Valve microactuators are located at both outlets. Teflon micro-tubing (o.d./i.d.: 1.6/1.0 mm) is connected to the channels, and then deionized (DI) water injected into the inlet using a syringe. When applying a 15 V dc bias to the right-hand side valve, as shown in Fig. 8(a), the DI water could flow only through the left outlet. After turning off the bias voltage, the right valve opened so that the water could pass through the right outlet, as shown in Fig. 8(b).

3.2. Microgripper

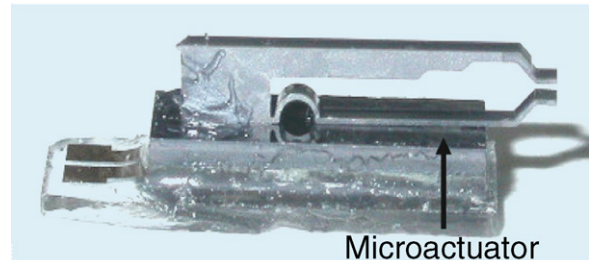
Two types of microgripper have been fabricated. One that can grip by activating the microactuator is termed ‘type-A’, as shown in Fig. 9(a), and the other that can ungrasp by activating the microactuator is termed ‘type-B’, as shown in Fig. 9(b). With type-A, the open distance between the two tips has been designed to be $300 \mu\text{m}$. Therefore, the target displacement of actuation is



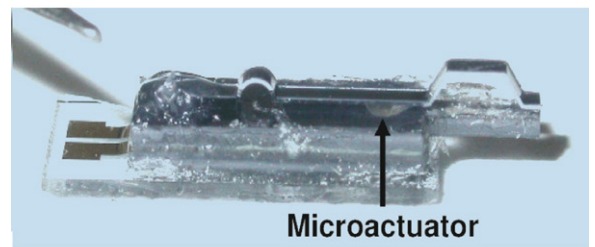
(a)



(b)



(c)



(d)

Fig. 7. Assembled devices: (a) microfluidic valve, (b) micropipette and microgripper of (c) type-A and (d) type-B.

at least $300 \mu\text{m}$, in order to fully close the microgripper. As shown in Fig. 9(a), when applying a bias of 10 V dc, the type-A microgripper is closed at the target distance. The type-B has been designed to open by $\sim 300 \mu\text{m}$. However, in practice, it only opens to $\sim 220 \mu\text{m}$ at the same bias, as shown in Fig. 9(b).

The height of the microgripper was measured at various dc bias voltages. With the type-A microgripper, the actuation height increased linearly with increasing voltage, as shown in Fig. 10. At a bias of 9 V, this microgripper is completely closed. However,

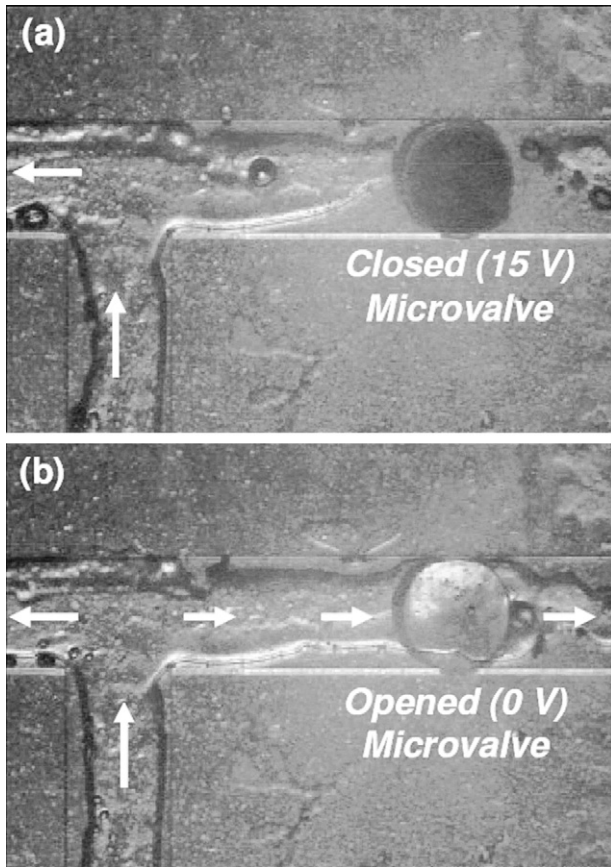


Fig. 8. Right-hand side of the microfluidic valve: (a) closed channel with 15 V dc applied to the microactuator and (b) opened channel with no bias.

even though type-B is actuated by the identical microactuator design used in type-A, it shows a different actuation characteristic. At a bias of 15 V dc, the actuation height reached $\sim 270 \mu\text{m}$. The difference in the actuation characteristics, between type-A and B, is likely to result from difference in the amount of paraffin wax, and dimensional variations in the microgripper designs, and unwanted air bubbles.

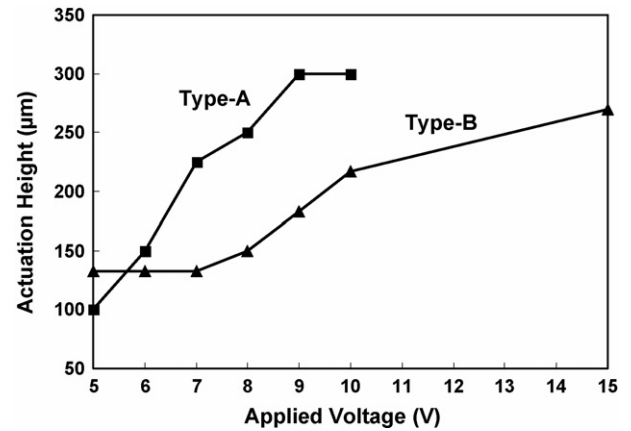


Fig. 10. Actuation height of the microgripper for type-A and type-B against applied dc voltages.

3.3. Micropipette

Another microfluidic application is the micropipette, realized using four microactuators integrated within the main chamber of the micropipette. The maximum volume of fluid that can be drawn is by activating all four microactuators at the same time. The expanded microactuators expel the air inside the chamber by applying 10 V dc bias. This creates a bubble at the tip of the glass micropipette, as shown in Fig. 11(a). In order to draw the fluid (in this case, DI water), the applied bias is turned off, to create a low pressure within the main chamber. Fig. 11(b) shows DI water being drawn into the micropipette. The maximum amount of drawn DI water was $6.74 \mu\text{l}$, by actuating all four microactuators. When biased to 10 V dc, for all four microactuators, all the DI water was expelled from the micropipette.

4. Calculating hydraulic pressure for expanding paraffin wax

The hydraulic pressure created by the expanding paraffin wax can be calculated using the measured deflection height, thickness

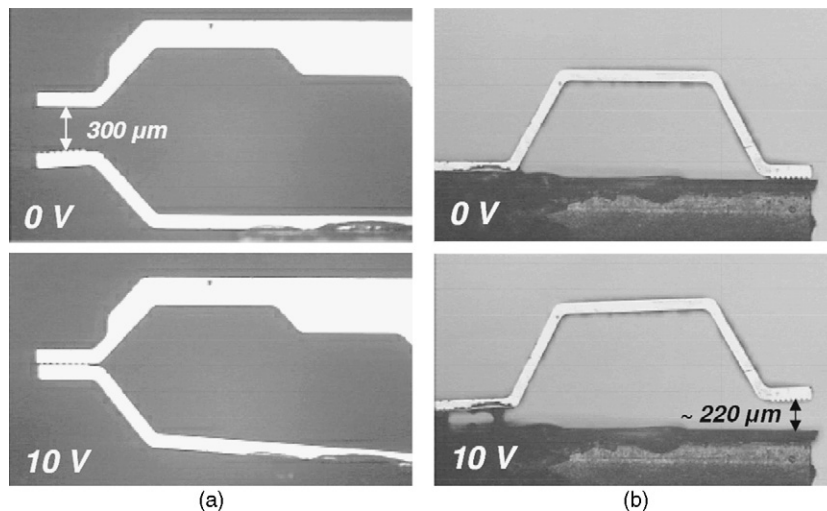


Fig. 9. Microgripper (a) type-A: open and closed with 10 V dc and (b) type-B: closed and opened with 10 V dc.

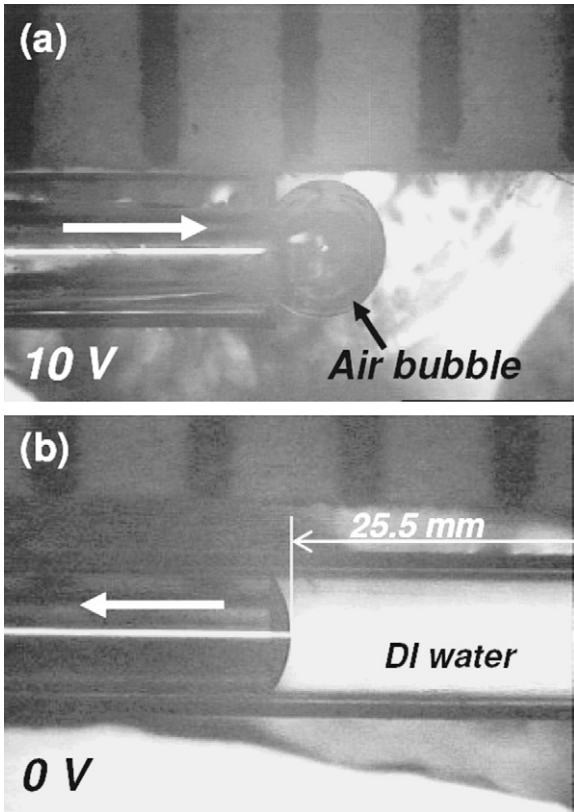


Fig. 11. Micropipette: (a) by applying a 10 V dc bias, the expelled air from the chamber creates an air bubble at the tip of the pipette and (b) the maximum drawn liquid after turning off the applied bias to all the microactuators.

and mechanical properties of the elastic diaphragm, according to the deflection theory for a circular plate. This theory is applied here, and for the first time, for the analysis of micromachined thin elastic diaphragms. There are two plate deflection theories: one is the small deflection theory, which deals with deflections of less than 25% of the diaphragm thickness; while the other is the large deflection theory, which is used for more than three times the deflection of the diaphragm thickness [10]. Using the measured deflection of the microgripper actuator, the hydraulic expansion pressure is calculated using the theory for large deflections of the diaphragm.

4.1. Clamped circular diaphragm deflection

When a circular diaphragm with a clamped edge is uniformly pressed by a pressure p_0 , as illustrated in Fig. 12, the small deflection of the circular diaphragm is given by [10]:

$$w(r) = \frac{p_0}{64D}(a^2 - r^2)^2 \tag{2}$$

The maximum deflection at the center ($r=0$) is given by:

$$w_{\text{center}} = \frac{p_0 a^4}{64D} \tag{3}$$

where p_0 and w are pressure and deflection of the diaphragm, respectively, and a and r are the radius of the diaphragm and

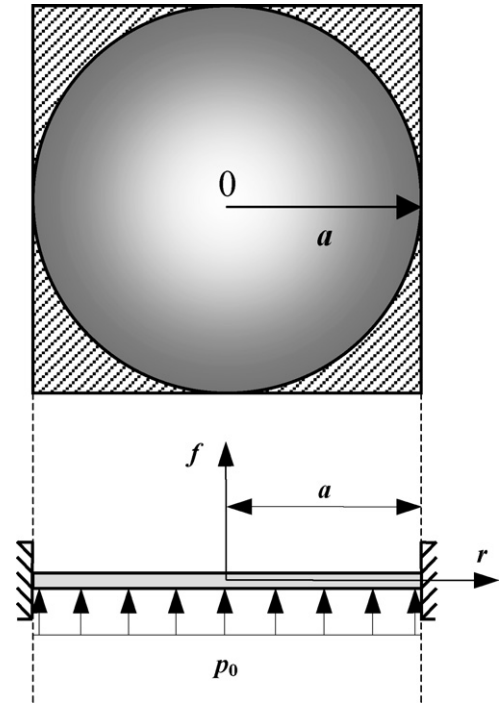


Fig. 12. Circular diaphragm with clamped edge and under uniform pressure.

radial coordinate, respectively. D is the flexural rigidity, given by:

$$D = \frac{Et^3}{12(1 - \nu^2)} \tag{4}$$

where E is Young’s modulus, ν the Poisson’s ratio and t is diaphragm thickness.

The large deflection of the diaphragm under the same conditions shown in Fig. 12 is given by [10]:

$$w(r) = f \left[1 - \left(\frac{r}{a} \right)^2 \right]^2 \tag{5}$$

where f is the maximum center deflection of the diaphragm. Therefore, at the center, the deflection is $w(0) = w_{\text{center}} = f$. The relationship between the maximum center deflection and the applied uniform pressure (p_0) is given as follow [11]:

$$p_0 = \frac{2Et(1 + \nu)(23 - 9\nu)}{21a^4(1 - \nu^2)} f^3 + \frac{16Et^3}{3a^4(1 - \nu^2)} f \tag{6}$$

Using the measured deflection f , the dimensions of the PDMS diaphragm of the microgripper microactuator (type-A) and the mechanical properties of the PDMS (given in Table 1), the expansion pressure of the paraffin wax can be calculated from (6). The measured values of a , t and f for this microgripper were 500, 77 and 300 μm , respectively. Fig. 13 shows deflec-

Table 1
Mechanical properties of PDMS [12]

Property	Value
Young’s modulus	0.868 MPa
Poisson’s ratio	0.5

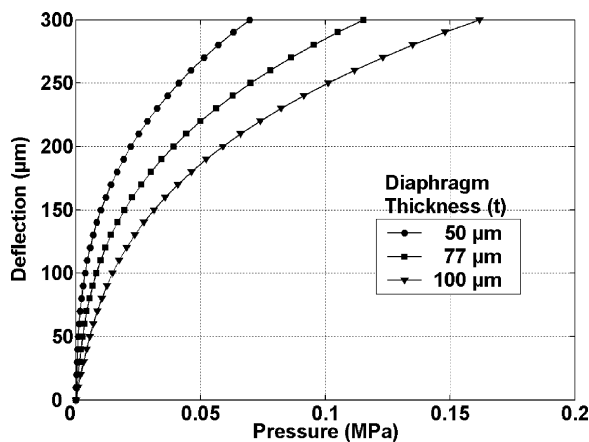


Fig. 13. Deflection against hydraulic pressure, for various thickness of PDMS diaphragm (maximum center deflection of 300 μm).

tions against hydraulic pressure, for different thicknesses of diaphragm. The calculated hydraulic pressure of the microactuator for microgripper type-A is approximately 0.12 MPa. As expected, it can be seen from Fig. 13 that a higher pressure is need to deflect a thicker diaphragm for the same height of deflection.

5. Conclusions

During melting, paraffin wax can generate large hydraulic forces by volumetric expansion. This hydraulic power has been exploited for the creation of a novel bulk-micromachined microactuator. To this end, we have demonstrated that this microactuator can be employed to realize a microfluidic valve, microgripper and micropipette. Each device has been assembled, using a novel material system that includes overglaze and PDMS, and successfully demonstrated. The microfluidic valve completely closed-off the DI water flow in the microchannel with a 15 V dc bias. Two types of microgripper have been demonstrated: type-A obtained the target actuation height of 300 μm , with a 10 V dc bias; while type-B opened to maximum actuation heights of between ~ 220 and ~ 270 μm , by applying 10 and 15 V dc bias voltages, respectively. The micropipette demonstrated a 6.74 μl sample of drawn DI water, which was subsequently expelled by applying a 10 V dc bias. Finally, for the first time, the hydraulic pressure of expanding paraffin wax was calculated using the theory of large deflections for a circular plate and measured data from the type-A microgripper. This pressure was approximately 0.12 MPa.

Acknowledgments

The authors would like to acknowledge Dr. John P. Stagg for undertaking the DRIE and Dr. Munir M. Ahmad for his advice on materials.

References

[1] P. Krulvitch, A.P. Lee, P.B. Ramsey, J.C. Trevino, J. Hamilton, M.A. Northrup, Thin film shape memory alloy microactuators, *IEEE J. MEMS* 5 (December (4)) (1996) 270–282.

[2] M. Freund, R. Csikös, S. Keszthelyi, G.Y. Mőzes, *Paraffin Products: Properties, Technologies Applications*, Elsevier, Amsterdam, 1982.

[3] S.F. Tibbitts, High-output paraffin linear motors: utilization in adaptive systems, *SPIE Proc.* 1543 (1991) 388–399.

[4] D.E. Downen, Design and implementation of a paraffin based micropositioning actuator, *SPIE* 3132 (1997) 127–134.

[5] N. Kabei, M. Kosuda, H. Kagamibuchi, R. Tashiro, H. Mizuno, Y. Ueda, K. Tsuchiya, A thermal-expansion-type microactuator with paraffin as the expansive material, *JSME Int. J. Ser. C* 40 (4) (1997) 736–742.

[6] E.T. Carlen, C.H. Mastrangelo, Electrothermally activated paraffin microactuators, *J. MEMS* 11 (June (3)) (2002) 165–173.

[7] L. Klintberg, M. Karlsson, L. Stenmark, J.-Å. Schweitz, G. Thornell, A large stroke, high force paraffin phased transition actuator, *Sens. Actuators A* 96 (2002) 189–195.

[8] E.T. Carlen, C.H. Mastrangelo, Surface micromachined paraffin-actuated microvalve, *J. MEMS* 11 (October (5)) (2002) 408–420.

[9] J.S. Lee, S. Lucyszyn, A micromachined refreshable Braille cell, *IEEE/ASME J. MEMS* (4) (2005) 673–682.

[10] S. Timoshenko, S. Woinosky-Krieger, *Theory of Plates and Shells*, McGraw Hill Classic Textbook Reissue, 1987.

[11] W.P. Eaton, F. Bitsie, J.H. Smith, D.W. Plummer, A new analysis solution for diaphragm deflection and its application to a surface-micromachined pressure sensor, in: *Int. Conference on Modelling and Simulation of Microsystems, MSM 99*, April 19–21, 1999.

[12] D. Armani, C. Liu, N. Aluru, Re-configurable fluid circuits by PDMS elastomer micromachining, in: *IEEE International Conference on Micro Electro Mechanical Systems*, January 17–21, January 1999, pp. 222–227.

Biographies

Jun Su Lee was born in South Korea in 1970. He received the MSc and PhD degree in metallurgical engineering from Yonsei University (Seoul, Korea) in 1999 and in electrical & electronic engineering from Imperial College London (UK) in 2006. From 2000 to 2001, he worked as an intern researcher, within the Metal Processing Research Centre of the Materials Science and Technology Division in the Korea Institute of Science and Technology (KIST, Seoul). His current interests are in intelligent materials for MEMS, microactuators, microsensors and microfluidic devices.

Stepan Lucyszyn joined Imperial College in June 2001, as a senior lecturer within the Optical and Semiconductor Devices Group. Prior to this, he was a senior lecturer at the University of Surrey, within the Microwave and Systems Research Group. His teaching, research and professional activities range from undertaking theoretical investigations to demonstrating experimental proof-of-concepts in many RF areas of applied physics (e.g., electromagnetics, photonics, materials, semiconductor devices) and engineering (e.g., component characterisation, synthesis/analysis, circuit design, fabrication and metrology) at microwave/millimetre-wave frequencies. Over the past 4 years, Dr. Lucyszyn has been teaching complete bespoke professional development short courses within S.E. Asia (on wireless systems, circuit design, advanced technologies, manufacture and metrology). These 1–5 days courses are aimed at graduates, academics and professional engineers. Following 12 years of RFIC/MMIC research, he has spent the past 5 years focusing on RF MEMS. He represents Imperial within the European Union's Framework VI Network of Excellence on Advanced MEMS for RF and Millimeter Wave Communications (AMICOM). During the summer of 2002, Dr. Lucyszyn worked as a guest researcher, within the MEMS laboratory of the National Institute of Advanced Industrial Science and Technology (Tsukuba, Japan). In 2004, he published a review paper on RF MEMS technology, which won an IEE Premium Award in 2005. More recently, in October 2005, he gave an invited presentation of his RF MEMS research activities to a NATO Workshop. In November 2005, he was appointed an associate editor and serves as a member of the Editorial Board for the *IEEE/ASME Journal of Microelectromechanical Systems*. To date, Dr. Lucyszyn has (co-)authored over 100 publications in areas of applied physics and engineering. In 2005, he was elected Fellow of the Institution of Electrical Engineers and a Fellow of the Institution of Physics.